# Defect generation and annihilation in hydrogenated amorphous silicon during plasma treatment

S. Nunomura, I. Sakata and K. Matsubara

*National Institute of Advanced Industrial Science and Technology (AIST), Tsukuba, Ibaraki 305-8568, Japan*

**Abstract:** We study the defect kinetics in hydrogenated amorphous silicon (a-Si:H) during hydrogen ($H_2$) and argon (Ar) plasma treatments. The generation and annihilation of electronic defects are monitored via in-situ photocurrent measurement. The defects are generated by the radical species such as H atoms for a $H_2$ plasma and metastable Ar atoms for an Ar plasma. The $Ar^+$ ion bombardment creates the residual defects. The residual defects are partially recovered by an additional $H_2$ plasma and postannealing treatment.

**Keywords:** defects, a-Si:H, photocurrent, $H_2$ plasma, Ar plasma, solar cells.

## 1. Introduction

Electronic defects in semiconductor devices play important roles in the device performance and reliability [1,2]. The defects are often generated during device fabrication, where a variety of plasma processing are used for thin-film deposition, etching, dopant implantation and surface modification. Most of the defects are annihilated by post-annealing. However, some defects remain in devices, restricting the device performance and reliability.

During plasma processing, the electronic defects can be generated near the material surface for several reasons (Fig. 1). The surface is exposed to ion bombardment, photon irradiation, and radical exposure. The ion bombardment leads to surface strain and loss of matter by sputtering events, which results in the formation of defects. Some energetic ions may penetrate into certain materials, where they are neutralized and behave as impurities. The photon irradiation generates dangling bonds by breaking the weak-bonds in materials. The radical exposure is expected to generate defects, by transferring the internal energy to the surface atoms and/or chemically reacting with the lattice atoms.

## 2. Experiment

We prepare samples with four different structures by placing glass or quartz over a-Si:H film. Sample A is an uncovered a-Si:H film, and the film is thus exposed to ions, radicals and photons generated by the plasma. Sample B is an a-Si:H film covered with glass and with a gap. The inclusion of the glass eliminates ion bombardment on the a-Si:H film. Sample C is an a-Si:H film covered with glass and sealed completely with ceramic paste. This prevents the exposure of the a-Si:H film to radicals, and the film. Sample D is an a-Si:H film covered with quartz glass and sealed with ceramic paste. The a-Si:H film is exposed to VIS, UV, and also vacuum UV (VUV) photons.

The plasma-treatment experiments are performed in capacitively coupled 60-Mhz VHF discharges in a parallel plate configuration[3,4]. The sample is placed on the electrically grounded electrode, and heated at a temperature $T$ in the range from 120 to 240 ◦C. Either $H_2$ gas or Ar gas is introduced into a vacuum chamber. The gas pressure is set at 0.3 Torr by regulating a gas flow rate of 50 sccm. The discharge is maintained by supplying a VHF discharge power $P_{VHF}$ ranging from 3W to 50 W.

A a-Si:H film is illuminated with a 520-nm-wavelength laser operated at 1 mW. The photon energy of the laser light hν is 2.38 eV, which is larger than the band gap of a-Si:H (1.70 eV). The photogenerated carriers are collected by the interdigitated contacts, which are biased at 10 V (dc) with respect to each other. The electrons are mainly collected by the contacts since the mobility of electrons is much larger than that of holes. The intensity of the laser light is modulated to 1.111 kHz, and the photocurrent signal oscillating at this frequency is extracted by a lock-in technique. The lock-in time constant is set at 100 ms. By use of this lock-in technique, the laser-induced photocurrent is distinguished from plasma-generated currents such as plasma-emission-induced photocurrent and ion current.

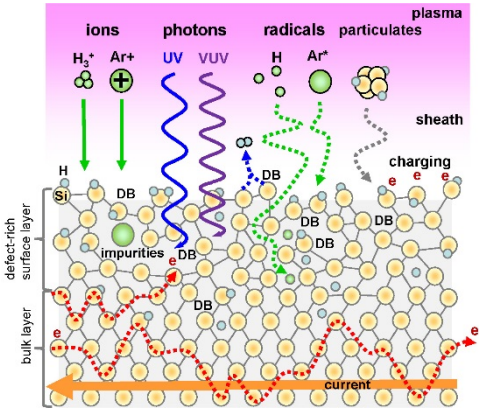


Fig. 1. Defect generation during plasma processing[5].

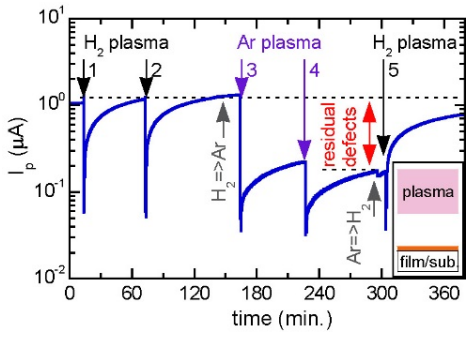


Fig. 2. Time evolution of photocurrent in a-Si:H film for sample A during plasma and post-annealing treatments [5].

## 3. Results & discussion

Figure 2 shows a time evolution of the photocurrent, $I_p$, in an a-Si:H film for sample A during the plasma treatments and postannealing [5]. We find that each $H_2$ and Ar plasma treatment causes a strong reduction in $I_p$, typically by one order of magnitude. The reduction in $I_p$ takes place immediately after initiating the discharge/treatment; the decay time of $I_p$ is less than 100 ms, which is limited by the lock-in time constant. The observed strong reduction indicates the generation of defects, i.e., the plasma-induced defects. Since $I_p \propto 1/n_d$, the defect density is expected to be increased by one order of magnitude during the plasma treatment.

Once the discharge/treatment is terminated, $I_p$ is increased with time, showing a defect recovery trend. Interestingly, this recovery behaviour of $I_p$ depends on either the $H_2$ or Ar plasma treatment performed before. For the $H_2$ plasma treatment, $I_p$ returns completely to the initial level after annealing. On the contrary, it does not return to the initial level for Ar plasma treatment; $I_p$ returns only 20 % of the initial level. The results suggest that the $H_2$ plasma-induced defects are annihilated completely by annealing, whereas the Ar plasma-induced defects are not, and some of these defects remain in the film. However, these remaining defects, i.e., the residual defects, are mostly annihilated by additional $H_2$ plasma and postannealing. This result suggests that the $H_2$ plasma treatment is beneficial for the annihilation of Ar plasma-induced residual defects.

Figure 3 shows an example for the time evolution of $I_p$ under the photon irradiation of a $H_2$ plasma at various discharge power [5]. From the experiments of the photon irradiation, we can make the following brief conclusions. Firstly, the VIS photons generate less defects than those of UV photons. Secondly, the UV photon-induced defects are increased with the UV photon flux. Thirdly, the photons do not create the residual defects; the photon-induced defects are annihilated completely by annealing.

Figure 4 shows an Arrhenius plot for the annihilation of defects [5]. The following results are found. Firstly, $1/\tau$ shows an exponential decay on $1/T$, indicating that a thermal activation process plays important roles in the defect annihilation. Secondly, the exponentially decaying

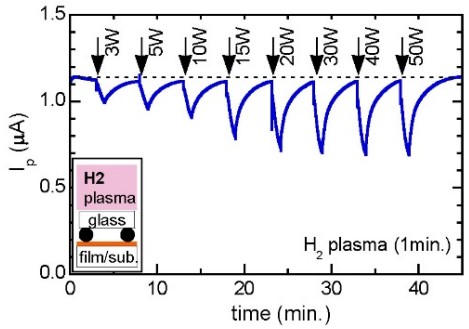


Fig. 3. Time evolution of $I_p$ in a-Si:H film for sample C during $H_2$ plasma UV photon irradiation [5].

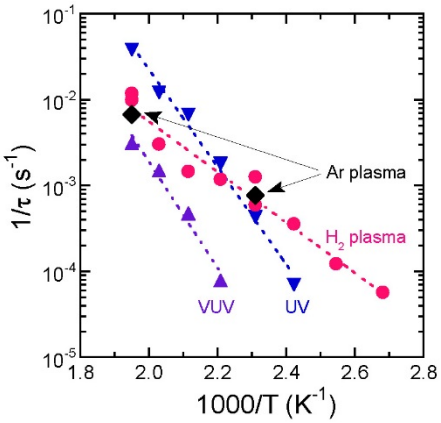


Fig. 4. Arrhenius plot for defect annihilation [5].

slope is different between the photon-induced and the plasma-induced defects; it is steeper for the photon-induced defects. To obtain the activation energy, $E_a$, the slope is fitted by

$$1/\tau = k_0 \exp(-E_a/k_BT). \quad (1)$$

We find $E_a$ =0.53±0.06 eV for the plasma-induced defects and $E_a$ = 1.17±0.06 eV for the photon-induced defects in a range of T = 120 – 240 °C. Thirdly, the values of $\tau$ are roughly the same between $H_2$ and Ar plasma-induced defects at a given T although the Ar plasma treatment causes the residual defects, and the $H_2$ plasma treatment does not. Fourthly, $k_0$ is different between the UV and VUV photon-induced defects while the activation energies are nearly the same between them; $k_0$ is smaller for the VUV photon-induced defects.

## 4. Summary

The kinetics of electronic defects in a-Si:H films is studied during $H_2$ and Ar plasma treatments, and postannealing. The generation and annihilation of the electronic defects, i.e, the silicon DBs, are successfully monitored via in-situ photocurrent measurements.


## Acknowledgments

The authors are grateful to Prof. M. Shiratani, Prof. K. Koga (Kyushu Univ.) and Dr. C. McDonald (AIST) for valuable discussions. This work is supported in part by JSPS KAKENHI (Grant Number 18K03603 and 15K04717).


## References


[1] S. Nunomura, X. Che, and S. R. Forrest, Adv. Mater. **26**, 7555 (2014).

[2] S. Nunomura, I. Sakata and K. Matsubara, J. Non-Cryst. Solids **44**, 436 (2016).

[3] S. Nunomura, I. Sakata, and M. Kondo, Appl. Phys. Express **6**, 126201 (2013).

[4] S. Nunomura and I. Sakata, AIP Adv. **4**, 097110 (2014).

[5] S. Nunomura, I. Sakata and K. Matsubara, Phys. Rev. Appl. **10**, 054006 (2018)